FULL-SCALE MSL HEATSHIELD MATERIAL RESPONSE USING DSMC AND CFD TO COMPUTE THE AEROTHERMAL ENVIRONMENTS

Arnaud Borner, Science and Technology Corporation at NASA Ames Research Center (arnaud.p.borner@nasa.gov)
Jeremie B.E. Meurisse, Science and Technology Corporation at NASA Ames Research Center (jeremie.b.meurisse@nasa.gov)
Nagi N. Mansour, NASA Ames Research Center (nagi.n.mansour@nasa.gov)

Introduction

During Mars atmospheric entry, the Mars Science Laboratory (MSL) was protected by a 4.5 meters diameter ablative heatshield assembled in 113 tiles [1]. The heatshield was made of NASA's flagship ablative material, the Phenolic Impregnated Carbon Ablator (**PICA**) [2]. Prior work [3] compared the traditional **one-dimensional and three-dimensional** material response models at different locations in the heatshield. It was observed that the flow was basically one-dimensional in the **nose and flank regions**, but three-dimensional flow effects were observed in the outer flank. Additionally, the effects of tiled versus monolithic heatshield models were also investigated. It was observed that the **3D tiled and 3D monolithic** configurations yielded relative differences for in-depth material temperature up to 18% and 28%, respectively, when compared to the a 1D model.

Aerothermal environments from SPARTA and DPLR

The MSL flight environment was simulated using the following assumptions for both the CFD and DSMC simulations:

- Super-catalytic wall BC: CO_2 and N_2 recombination to freestream mole fractions
- Radiative equilibrium wall with $\varepsilon = 0.89$
- Mars atmosphere $y_{CO2} \approx 0.97$ and $y_{N2} \approx 0.03$
- 8 species and 24 reactions(12 forward + 12 backward): Mitcheltree model [6]
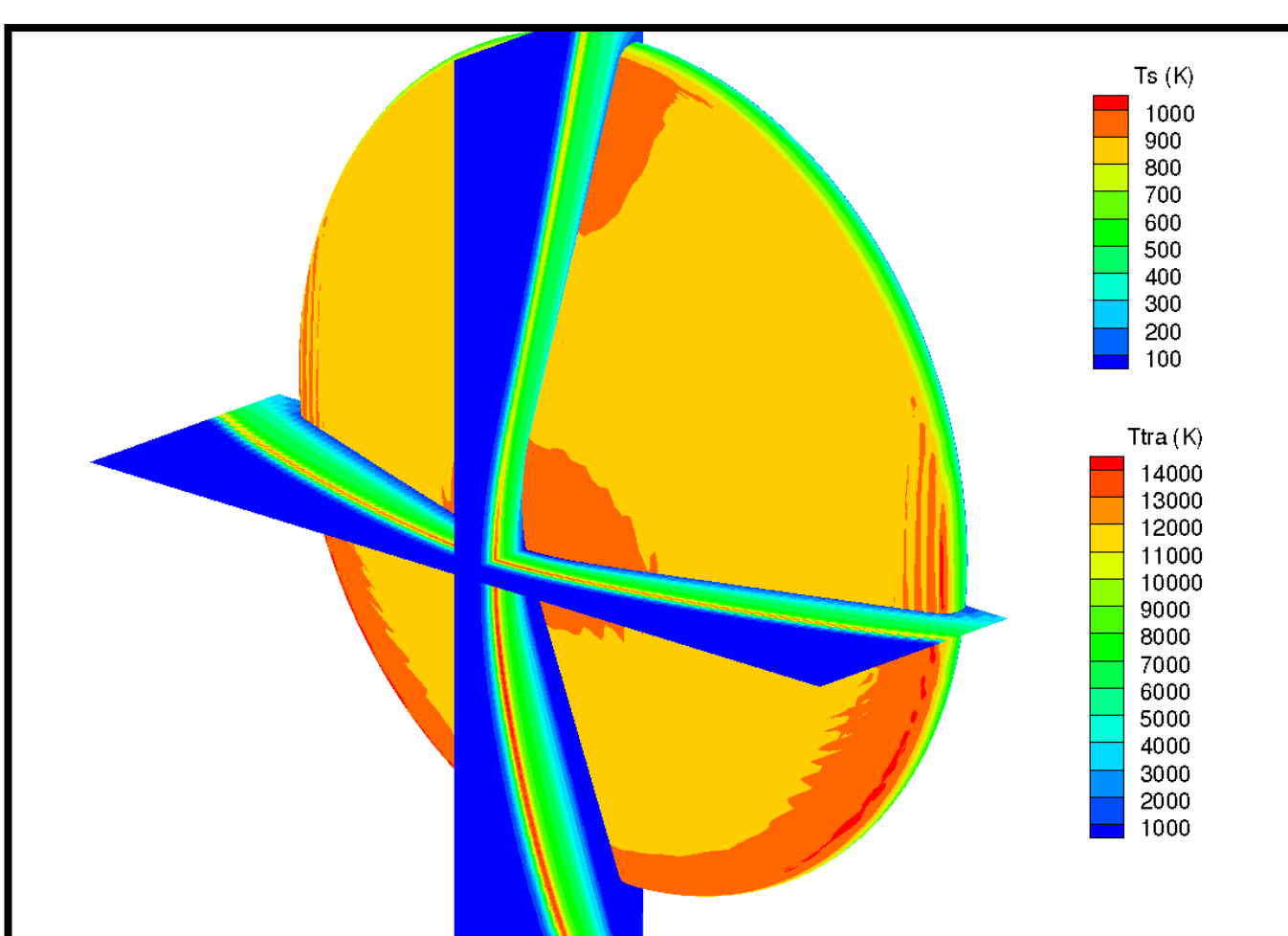- Park hypersonics correction to vibrational relaxation

DSMC

The objective of this work is to study the effects of the aerothermal environment on the material response. We extend prior work [3] by computing aerothermal environments using the direct simulation Monte Carlo (**DSMC**) code **SPARTA** [4] and the CFD code Data Parallel Line Relaxation (**DPLR**) [5]. SPARTA is used to compute environment in the **rarefied regime** prior to 48.4s of entry where the **Knudsen number** is such that the Navier-Stokes equations can be inaccurate. Similarly to previous work, the DPLR software is used to compute the hypersonic environment for a laminar boundary layer assumption from **48.4 s up to 100 s** after Entry Interface (EI) along the MSL 08-TPS-02/01a trajectory.

SPARTA: https://sparta.sandia.gov
DPLR: https://software.nasa.gov/software/ARC-16021-1A
PATO: https://software.nasa.gov/software/ARC-16680-1

Differences between CFD and DSMC:
- DPLR uses a 2 temperature model and SPARTA a 3 temperature model
- Laminar boundary layer model in DPLR
- Binary diffusion coefficients from Gupta collision integrals [7] in DPLR
- SPARTA uses Variable Soft Sphere (VSS) model with high temperature transport calibration
- Parker equation for rotational relaxation and Millikan-White equation + Park correction for vibrational relaxation in SPARTA

Fig. 1 Surface and translational temperature contours at 40 s of entry computed using DSMC

- Shock standoff distance decreases with decreasing altitude
- Strong non-equilibrium in shock at high altitudes
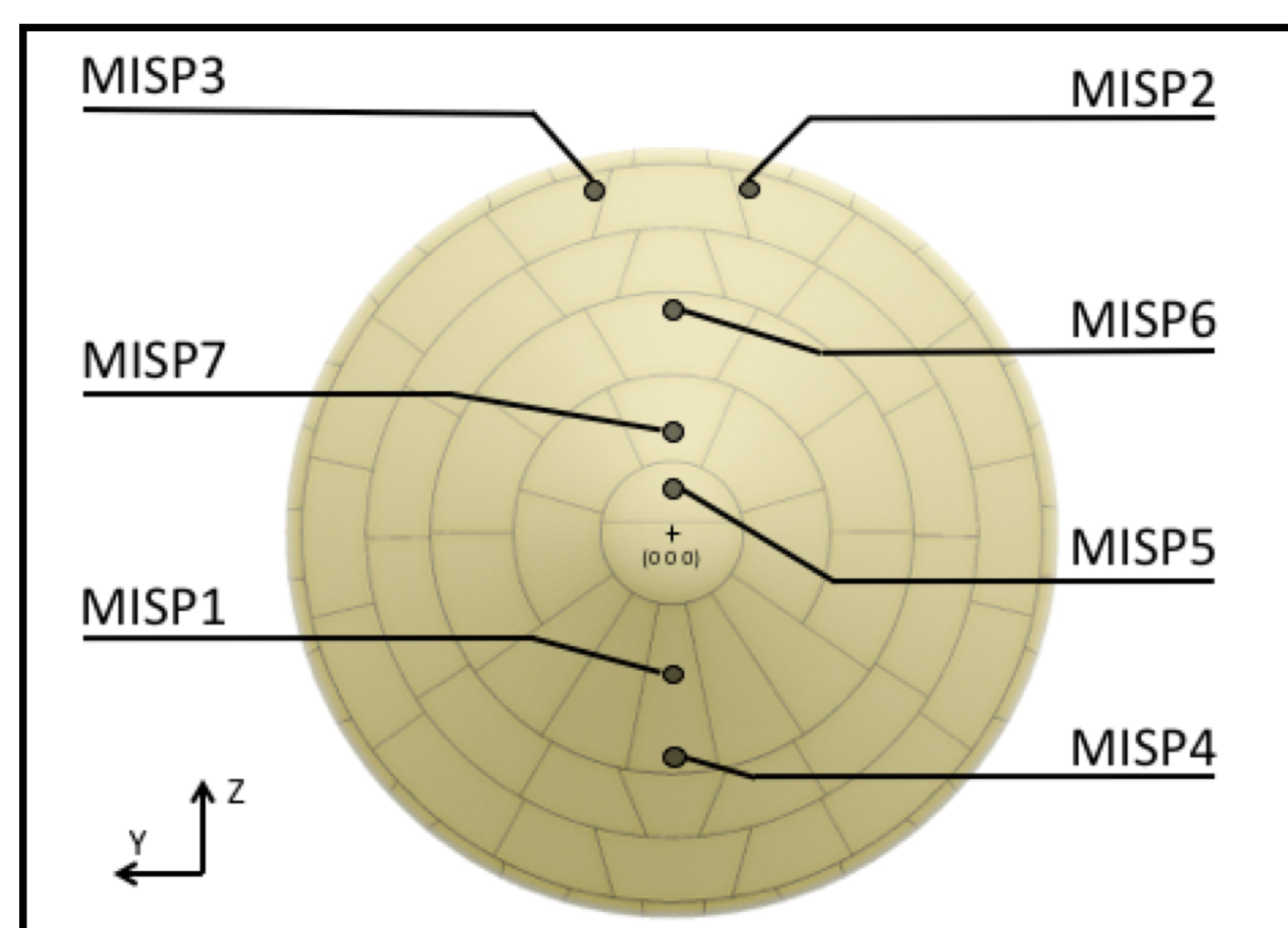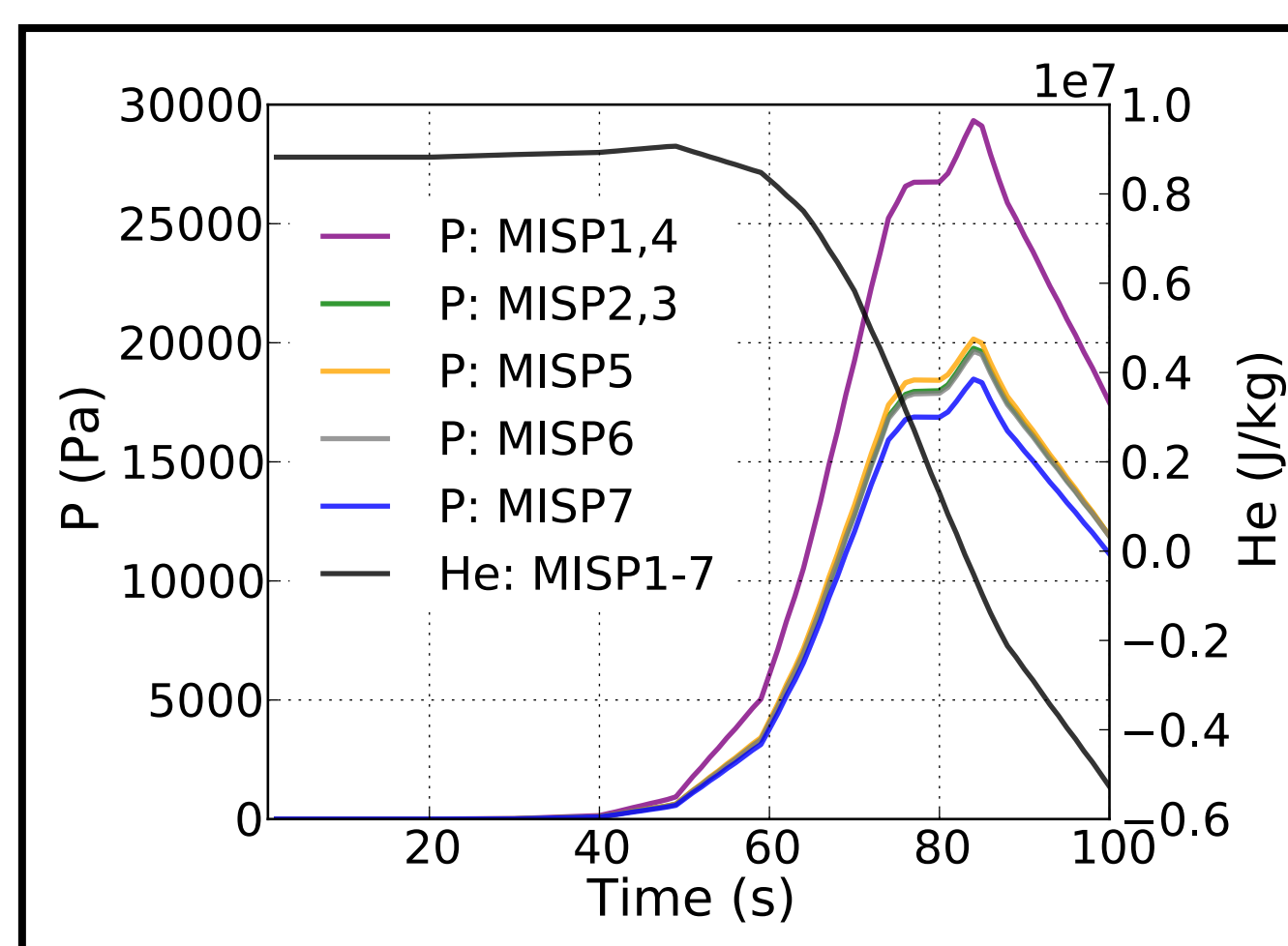- Angle of attack varies from 30 deg at high altitude to 16 deg after 48 s of entry

Fig. 2 MEDLI Integrated Sensor Plug (MISP) locations [3]

- 7 plugs with 4 thermocouples each
- Nominal depth: TC1: 2.54 mm, TC2: 5.08 mm, TC3: 11.43 mm, TC4: 17.78 mm [8]
- MISP4 located at the stagnation point
- Assembly of 113 PICA tiles
- TACOT material properties used in PATO

Fig. 3 Evolution in time of pressure (p_w) and BLE enthalpy (h_e) at the front surface

- Peak of pressure occurs around 84 s, highest at plugs 1 and 4, close to stagnation point
- BLE enthalpy is high until 60 s then sharply drops to negative values after 84 s
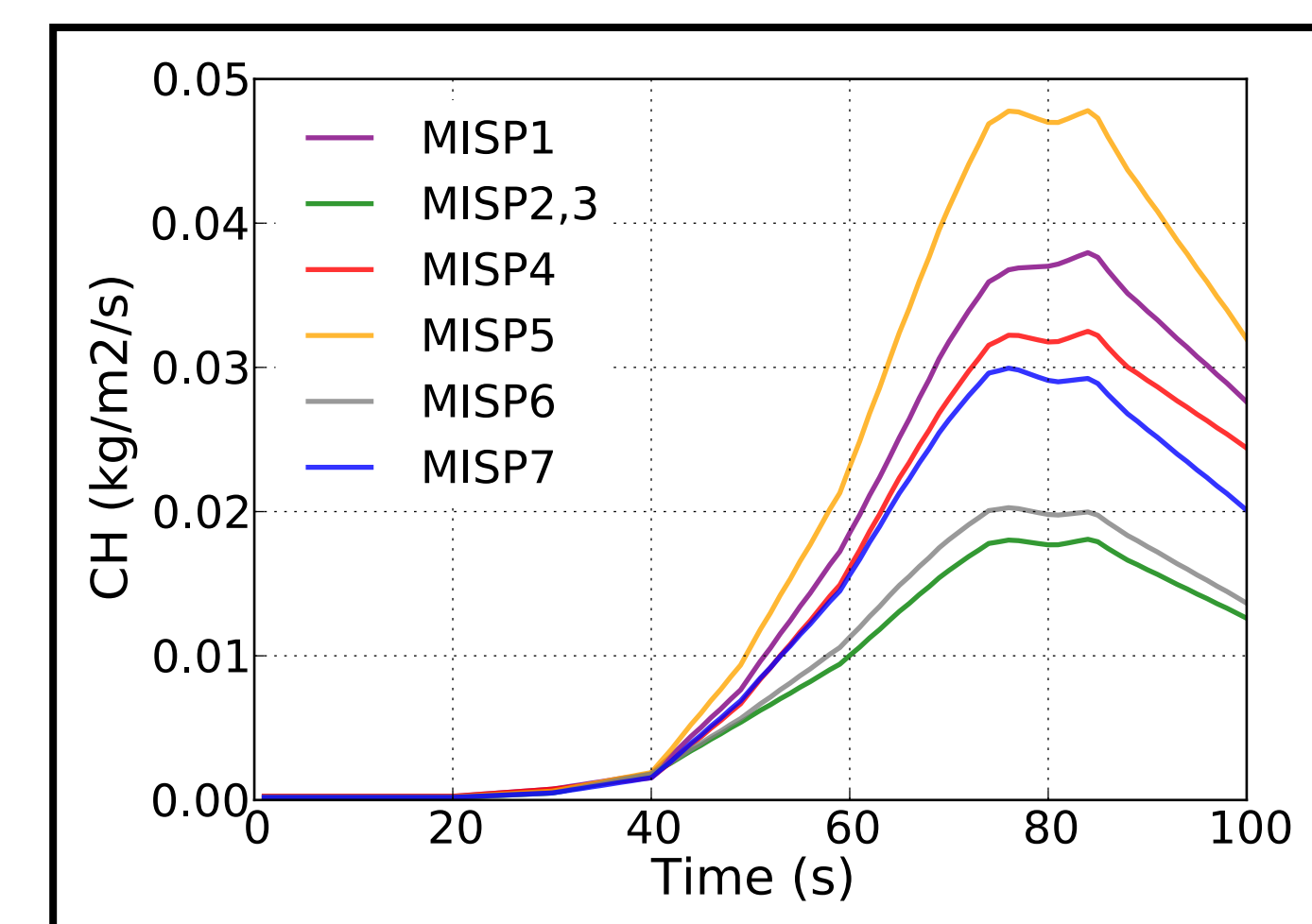

Fig. 4 Evolution in time of heat transfer coefficient (C_H)at the front surface

- C_H computed from PATO Boundary Layer utility and BLAYER [9] as ratio of q_w to (h_e-h_w)
- Two peaks in heat transfer coefficient appear around 75 s and 85 s
- Maximum heating occurs at MISP5

Material response from PATO

The Porous material Analysis Toolbox based on OpenFOAM (**PATO**) [10, 11] is used for the material response calculations. The governing equations are volume-averaged forms of solid mass, gas mass, gas momentum and total energy conservation, including pyrolysis gas production. The thermodynamics and chemistry properties are computed using the **Mutation++** library [12]. The boundary conditions at the heatshield front surface are interpolated in time and space from the aerothermal environment at discrete points of the MSL trajectory [3], using a Galerkin projection. For this study, the Theoretical Ablative Composite for Open Testing (**TACOT**) database developed by the TPS community was used to define the porous material properties. TACOT is a fictitious material that was inspired from low density carbon/phenolic ablators. The boundary layer edge (BLE) quantities from DPLR are extracted using a curvature-based method with the **BLAYER** code [9]. For the DSMC results, a Boundary Layer utility was created in PATO and an edge-based method is used (location of BLE such that h_e = 99.5 % of h_∞). At 40 s after EI, the peak pressure value computed from **SPARTA** is reached in the stagnation point region (MISP4) around 150 Pa (Fig. 5). We compute the PATO material response of the MSL heatshield in a **monolithic 3D configuration**, with the Martian aerothermal environments derived from **DPLR only** and **DSMC+DPLR**. For both cases, a uniform initial temperature is imposed. The addition of the DSMC results modifies the **temperature prediction** for the first 60 s after EI (Fig. 6). For MISP4, in-depth thermal effects are as important as surface thermal effects especially before 60 s (Fig. 7). Fig. 8 shows the **surface recession** computed in PATO with the highest recession at MISP5 as expected for a **laminar aerothermal environment**. Almost no recession is observed before 60 s due to the low heat flux. Only subtle differences in the recession are found between DPLR only and DSMC+DPLR derived environments.
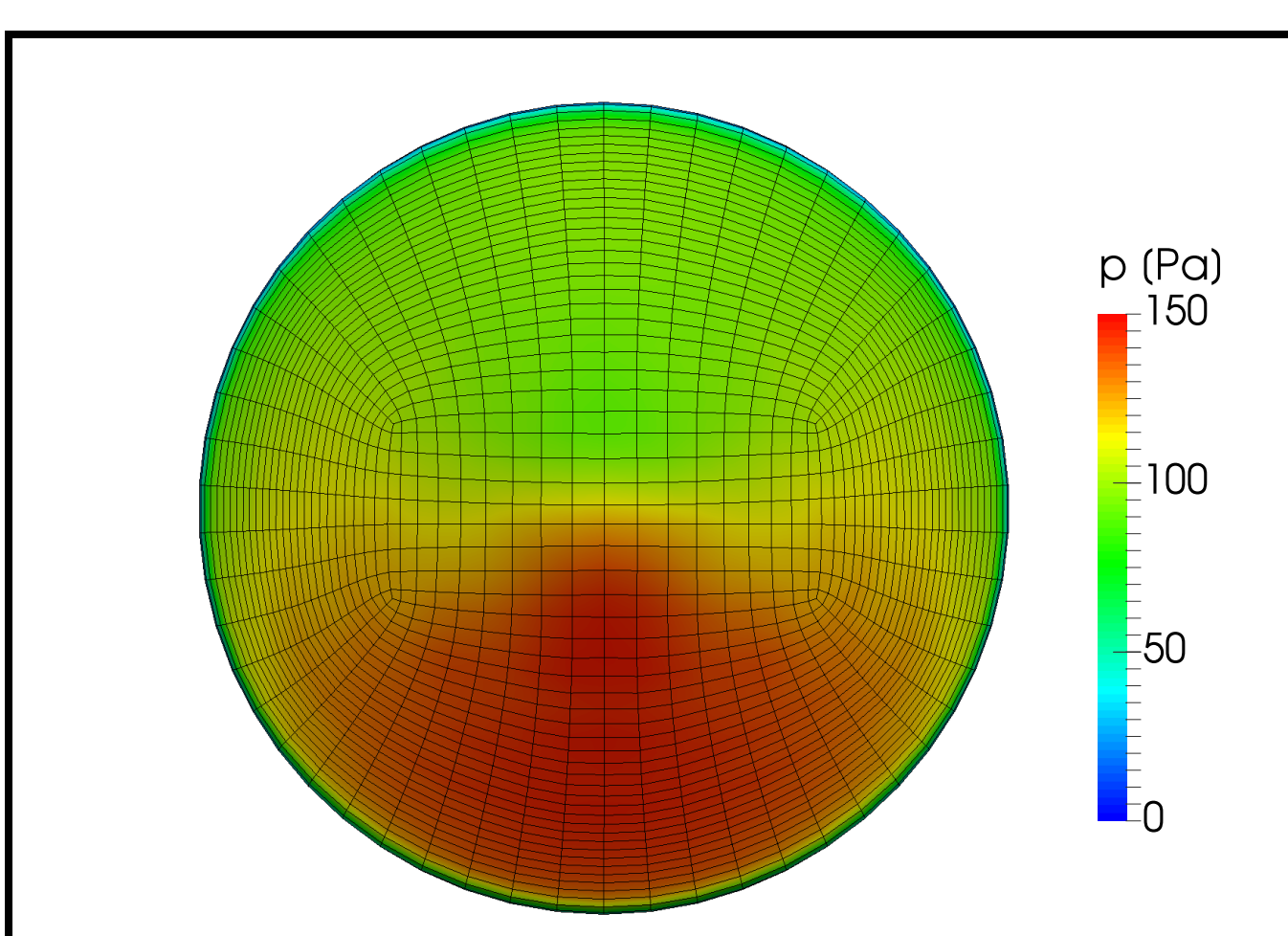

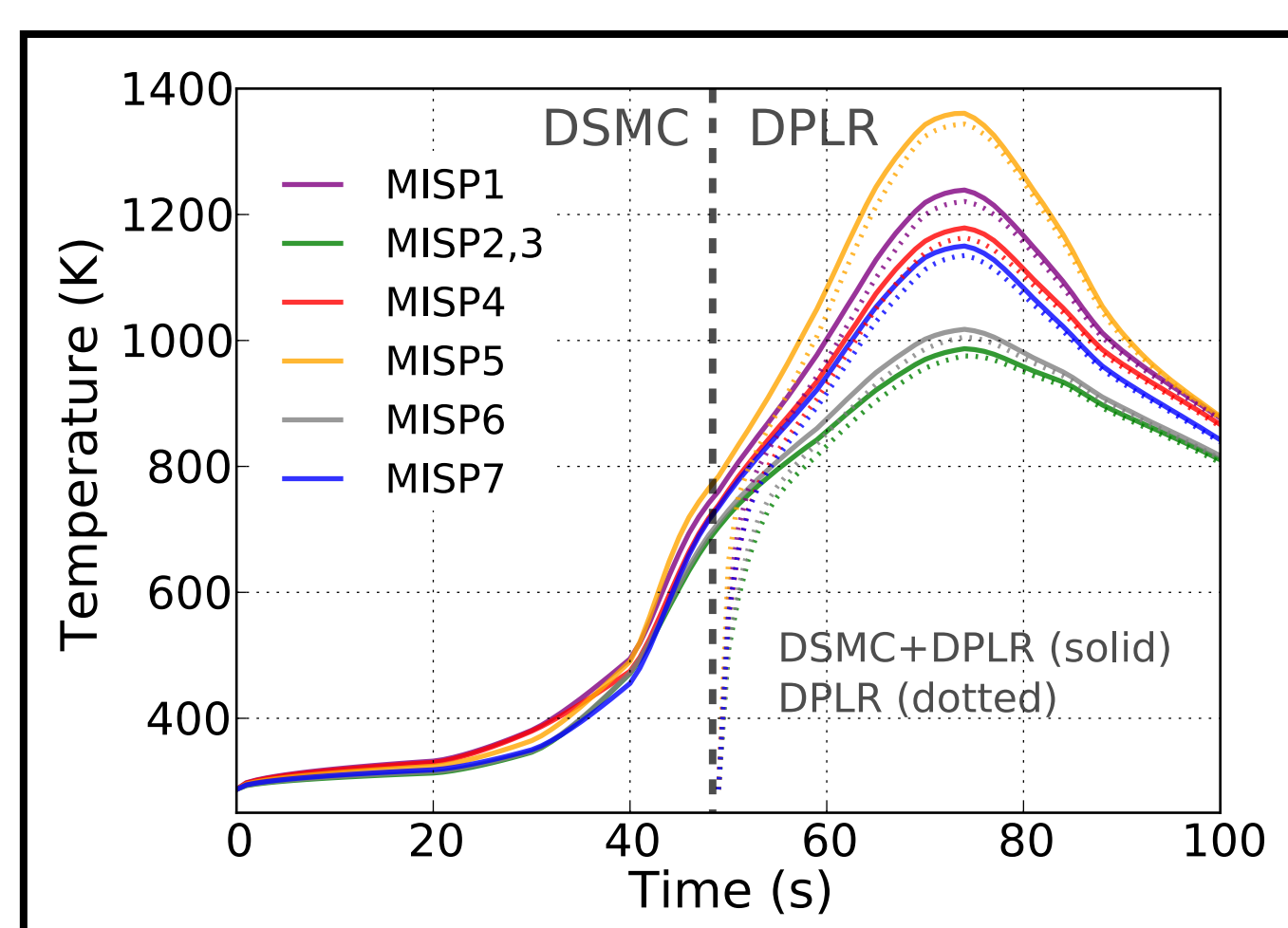**Fig. 5 3D-view of PATO input (pressure p_w) heat shield front surface (40s of MSL entry)**

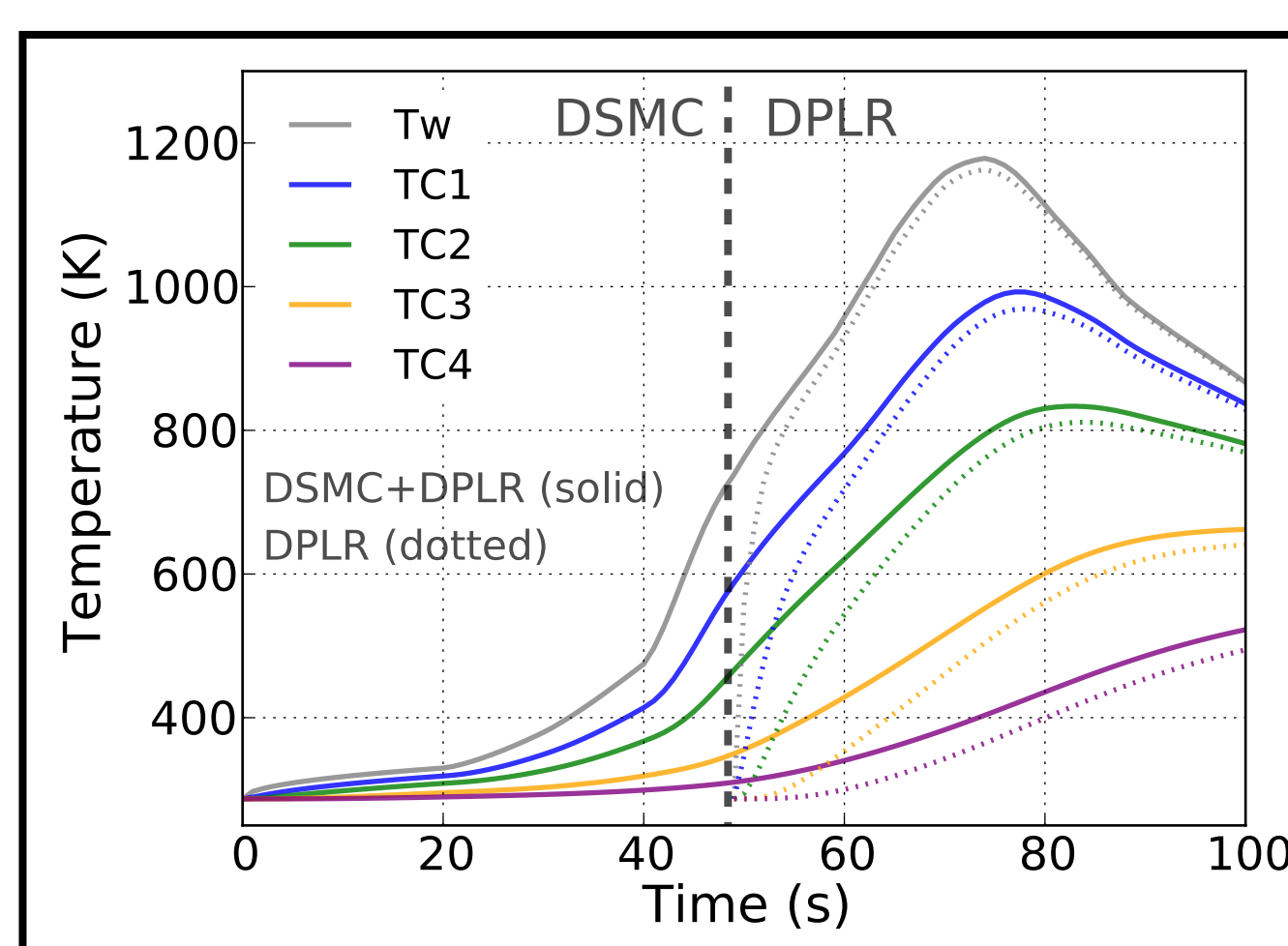**Fig. 6 PATO surface thermal response at the MISP locations**

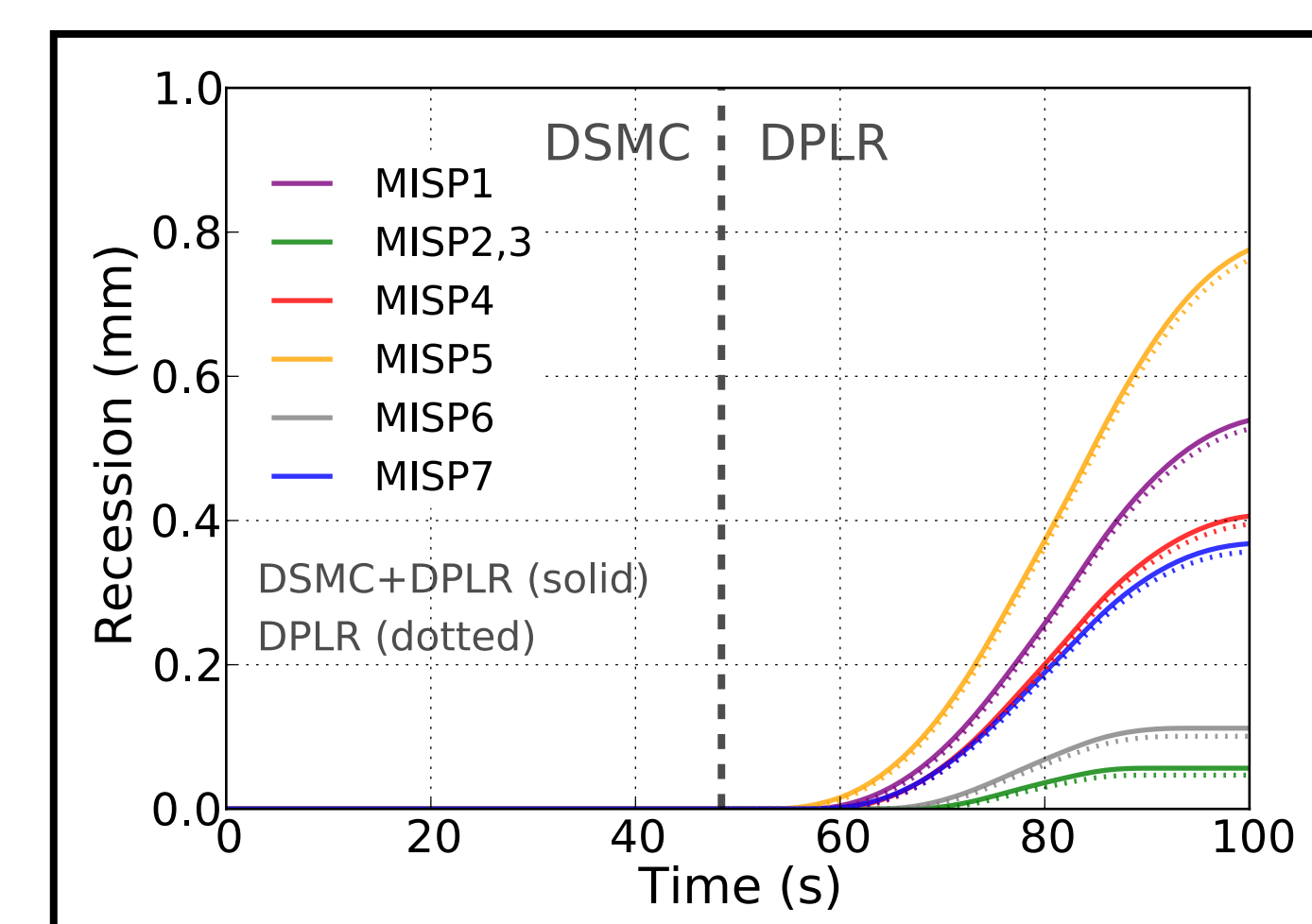**Fig. 7 PATO surface and in-depth thermal response at MISP4**

Fig. 8 PATO surface recession at the MISP locations

References

[1] K. T. Edquist, et al. (2009) *AIAA Paper* 2009-4075.
[2] M.J. Wright et al. (2009) *AIAA Paper* 2009-4231.
[3] J. B.E. Meurisse et al. (2018), *Aerosp Sci Technol*, 76, 497-511.

[4] M. A. Gallis et al. (2014), *AIP Conf Proc* 1628, 27.
[5] M. J. Wright et al. (2009), *DPLR Code User Manual: Acadia-Version 4.01.1.*
[6] R. Mitcheltree et al. (1995), *JSR* 32 (5), 771-776.
[7] R. Gupta et al. (1990), *NASA-RP*-1232.
[8] T. R. White et al. (2013), *AIAA Paper* 2013-2779.

[9] D. Saunders and D. Prabhu. (2018), *BLAYER User Guide,* NASA/TM-2018-219749.
[10] J. Lachaud and N. N. Mansour (2014), *J Thermophys Heat Tran,* 28, 191–202.
[11] J. Lachaud et al. (2017), *Int J Heat Mass Tran,* 108, 1406–1417.
[12] J. B. Scoggins and T. E. Magin (2014), *AIAA Paper* 2014-2966.